

Ionic Conductance Pathways in the Mouse Medullary Thick Ascending Limb of Henle

The Paracellular Pathway and Electrogenic Cl⁻ Absorption

STEVEN C. HEBERT and THOMAS E. ANDREOLI

From the Division of Nephrology, Department of Internal Medicine, University of Texas Medical School, Houston, Texas 77225

ABSTRACT Net Cl⁻ absorption in the mouse medullary thick ascending limb of Henle (mTALH) involves a furosemide-sensitive Na⁺:K⁺:2 Cl⁻ apical membrane symport mechanism for salt entry into cells, which occurs in parallel with a Ba⁺⁺-sensitive apical K⁺ conductance. The present studies, using the in vitro microperfused mouse mTALH, assessed the concentration dependence of blockade of this apical membrane K⁺-conductive pathway by Ba⁺⁺ to provide estimates of the magnitudes of the transcellular (G_c) and paracellular (G_s) electrical conductances (millisiemens per square centimeter). These studies also evaluated the effects of luminal hypertonicity produced by urea on the paracellular electrical conductance, the electrical Na⁺/Cl⁻ permselectivity ratio, and the morphology of in vitro mTALH segments exposed to peritubular antidiuretic hormone (ADH). Increasing luminal Ba⁺⁺ concentrations, in the absence of luminal K⁺, produced a progressive reduction in the transcellular conductance that was maximal at 20 mM Ba⁺⁺. The Ba⁺⁺-sensitive transcellular conductance in the presence of ADH was 61.8 ± 1.7 mS/cm², or ~65% of the total transepithelial conductance. In phenomenological terms, the luminal Ba⁺⁺-dependent blockade of the transcellular conductance exhibited negative cooperativity. The transepithelial osmotic gradient produced by luminal urea produced blebs on apical surfaces, a striking increase in shunt conductance, and a decrease in the shunt Na⁺/Cl⁻ permselectivity (P_{Na}/P_{Cl}), which approached that of free solution. The transepithelial conductance obtained with luminal 800 mM urea, 20 mM Ba⁺⁺, and 0 K⁺ was 950 ± 150 mS/cm² and provided an estimate of the maximal diffusion resistance of intercellular spaces, exclusive of junctional complexes. The calculated range for junctional dilution voltages

Address reprint requests to Dr. T. E. Andreoli, Dept. of Internal Medicine, The University of Texas Health Science Center at Houston, 1.150 Medical School Main Bldg., P.O. Box 20708, Houston, TX 77225. Dr. Hebert's present address is Renal Division, Brigham and Women's Hospital, 75 Francis St., Boston, MA 02115.

owing to interspace salt accumulation during ADH-dependent net NaCl absorption was 0.7–1.1 mV. Since the V_e accompanying ADH-dependent net NaCl absorption is 10 mV, lumen positive, virtually all of the spontaneous transepithelial voltage in the mouse mTALH is due to transcellular transport processes. Finally, we developed a series of expressions in which the ratio of net Cl^- absorption to paracellular Na^+ absorption could be expressed in terms of a series of electrical variables. Specifically, an analysis of paired measurement of $P_{\text{Na}}/P_{\text{Cl}}$ and G_s was in agreement with an electroneutral $\text{Na}^+:\text{K}^+:2 \text{Cl}^-$ apical entry step. Thus, for net NaCl absorption, ~50% of Na^+ was absorbed via a paracellular route.

INTRODUCTION

The purposes of this paper are to characterize further the transcellular and paracellular ionic conductance pathways in isolated mouse medullary thick ascending limbs of Henle (mTALH) exposed to antidiuretic hormone (ADH), and to evaluate the contributions of cellular and paracellular pathways to the spontaneous transepithelial voltage (V_e) accompanying net NaCl absorption. A model that has been set forth (Murer and Greger, 1982; Hebert and Andreoli, 1984*b*) to account for net NaCl absorption and net K^+ secretion in the mammalian TALH has proposed that net NaCl entry across apical membranes involves an electroneutral $\text{Na}^+:\text{K}^+:2 \text{Cl}^-$ symport process that occurs in parallel with a luminal K^+ conductance that recycles K^+ from cells to luminal fluids and serves as the route for net K^+ secretion. We have also proposed that, in the mouse mTALH, net Cl^- efflux across basolateral membranes is rheogenic (Hebert et al., 1984).

Our earlier evaluations (Hebert et al., 1984; Hebert and Andreoli, 1984*c*) of the electrical characteristics of the isolated mouse mTALH indicated, in accord with suggestions for other renal diluting segments (Guggino et al., 1982; Oberleithner et al., 1982*a, b*; O'Neil, 1983; Greger and Schlatter, 1983*a, b*), that apical plasma membranes of the mouse mTALH are predominantly, if not exclusively, K^+ selective. The combination of luminal Ba^{++} (in the range 1–5 mM) and 0 luminal K^+ produced graded reductions in transepithelial conductance (G_e) that were reversed competitively with increasing luminal K^+ concentrations (Hebert et al., 1984). However, these data provided no information about whether the combination of luminal Ba^{++} , in the range 1–5 mM, together with 0 luminal K^+ , produced a complete blockade of the transcellular pathway or, put differently, about the precise contribution of transcellular conductance to G_e . Nor have the studies cited above described the kinetic characteristics of luminal Ba^{++} , 0 K^+ blockade of transcellular conductance.

In the present experiments, we assessed the concentration dependence of the luminal Ba^{++} blockade of the transcellular conductance pathway. In phenomenological terms, the luminal Ba^{++} -dependent blockade of transcellular conductance, and hence of apical K^+ channels, exhibited negative cooperativity; with luminal 0 K^+ , 20 mM Ba^{++} , there was virtually complete blockade of the transcellular conductive pathway.

These data were also intended to provide a frame of reference for studies designed to assess the origin of the spontaneous lumen-positive transepithelial

voltage (V_e) accompanying net NaCl absorption in the mTALH. It is currently not possible to estimate accurately the true short-circuit current across isolated, microperfused mammalian renal tubular segments having transepithelial electrical conductances in the range of 100 mS/cm² (Greger, 1981; Hebert and Andreoli, 1984c; Hebert et al., 1984). Rather, the notion that V_e in the mouse mTALH might be rheogenic has depended, in part, on the observation that the equivalent short-circuit current is approximately equal to the sum of the chemically determined net rates of K⁺ secretion and Cl⁻ absorption (Hebert et al., 1984). However, the assignment of an electrogenic V_e for salt absorption processes in the mTALH also requires that lateral intercellular spaces be in virtual diffusion equilibrium with peritubular solutions (Hebert et al., 1981b).

One approach to evaluating the diffusion resistance of intercellular spaces exclusive of junctional complexes arises from the observations that, in hydraulically tight epithelia, luminal hypertonicity and the attendant bath-to-lumen osmotic gradient produce both a decline in transepithelial electrical resistance and a rise in the water and nonelectrolyte permeability of junctional complexes (Frömter and Diamond, 1972; Lindley et al., 1964; Ussing and Windhager, 1964; Ussing, 1966; DiBona and Civan, 1973; Schafer et al., 1974; de Bermudez and Windhager, 1975) and alterations in the structure of junctional complexes that are thought to represent a mechanical disruption of the latter (Erlj and Martinez-Palomo, 1972; DiBona, 1978).

Thus, we also evaluated the effects of luminal hypertonicity produced by urea on the properties of mTALH segments in which G_c was blocked by luminal Ba⁺⁺. These results indicate that the transepithelial osmotic gradient referable to luminal urea produced a morphological deformation of the apical surfaces of the mTALH segments, a striking increase in the shunt conductance, G_s , and an Na⁺/Cl⁻ permselectivity ratio which approached that of free aqueous solution. With 800 mM luminal urea, luminal 20 mM Ba⁺⁺, and 0 K⁺, the transepithelial electrical conductance provided a maximal estimate of the diffusion resistance of paracellular spaces, exclusive of junctional complexes. Our calculations, using these data, indicate that the diffusion resistance of intercellular spaces, exclusive of junctional complexes, was sufficiently small that, during net salt absorption, dilution voltages across the shunt pathway made a negligible contribution to V_e .

Finally, we developed a series of expressions in which the ratio of net transcellular Cl⁻ absorption to paracellular Na⁺ absorption could be expressed, given an electrogenic V_e , in terms of a series of transepithelial electrical variables; in turn, the latter were determined in paired observations on a series of mTALH tubule segments. The results were in agreement with the stoichiometric requirement for an electroneutral Na⁺:K⁺:2 Cl⁻ apical entry step.

MATERIALS AND METHODS

The basic techniques used in this laboratory for dissecting and perfusing single mTALH segments isolated from mouse kidneys have been described in detail previously (Hebert et al., 1981a, 1984); similar methodologies were used in the present studies. Stated briefly, 20–30-d-old male Swiss white mice were killed by cervical dislocation, decapitated, and rapidly exsanguinated. The kidneys were removed, sectioned into quarters, and then placed in cold (5°C) HEPES-buffered control bathing solution. Segments of medullary

thick ascending limbs, 0.2–0.4 mm in length, were dissected from the outer medullary area (see Hebert et al., 1981a, for a detailed description). After the medullary thick limb segments were transferred to a plastic perfusion chamber fitted to the stage of an inverted microscope (Zeiss IM 45), they were perfused using two sets of concentric glass pipettes (see below for details of perfusion pipettes) at rates between 10 and 20 nl/min. These perfusion rates are sufficient to minimize axial changes in the perfusate ion concentrations, and thus to minimize variations in the spontaneous transepithelial voltage along the length of the tubule (Hebert et al., 1981b). The perfusion chamber used in the present experiments permitted bathing solutions to flow continuously through the chamber at rates of 15–20 ml/min, after having been equilibrated with 100% O₂ and warmed to 37 ± 0.50°C (Hebert et al., 1984a).

Composition of Solutions

For control periods, we used a standard HEPES-buffered solution containing (mM): 140 NaCl, 5.0 KCl, 1.0 CaCl₂, 1.2 MgCl₂, and 3.0 HEPES (Hebert et al., 1984). The perfusing and bathing solutions were identical except for the addition of 5.5 mM glucose and 0.4 gm/100 ml of exhaustively dialyzed bovine serum albumin to the bathing solutions and an equiosmotic concentration of urea to the perfusion solutions. All solutions were adjusted to an osmolality of 295–300 mosmol/kg H₂O and a pH of 7.40 after equilibration with 100% O₂. HEPES was used as the buffer in all experiments in order to avoid anions that might form precipitates with Ba⁺⁺, an especially critical maneuver when using solutions containing >5 mM Ba⁺⁺. CO₂ and HCO₃⁻, which were excluded from external solutions, are not required to maintain ADH-dependent NaCl absorption in this nephron segment (Hebert et al., 1981a).

Barium, where indicated, was added to the perfusate in the form of BaCl₂. No ion substitutions were made for barium concentrations of <1.0 mM; however, in order to avoid significant luminal hypertonicity effects (Hebert et al., 1981c; Hebert and Andreoli, 1984c), barium replaced an equal concentration of NaCl when higher barium concentrations (5–20 mM) were used. Reductions in perfusate NaCl concentrations of this magnitude had no appreciable effect on G_e. Increases in perfusate and/or bath osmolality were made with urea where indicated. Salt dilution voltages across the mTALH were obtained using bathing solutions in which the NaCl concentrations were reduced to 50 mM and replaced equiosmotically with mannitol.

ADH (synthetic arginine vasopressin, grade V, Sigma Chemical Co., St. Louis, MO) was added to all bath solutions at 10 μU/ml, a concentration that produces a maximal increase in both the transepithelial voltage and the rate of NaCl absorption in the mouse mTALH (Hebert et al., 1981a). Furosemide was kindly provided by Hoechst Pharmaceuticals, Somerville, NJ.

Electrical Measurements

The electrical circuit used for the present experiments was identical to that described previously (see Fig. 1 in Hebert et al., 1984), except that a modified current-voltage clamp (VCC 600, Custom Control, Houston, TX) was used as the high-impedance differential amplifier for current-passing and voltage measurement. The perfusion pipette was formed from 2-mm electrode glass that was divided axially by a glass septum (theta-glass), thus permitting a virtually complete electrical separation of the perfusion and current-passing circuits (see Hebert et al., 1984a, for details). The perfusion half of the theta-glass pipette was fitted with an exchange pipette through which the perfusate was continuously flushed at 5–10 ml/min. This open-ended system allowed the perfusate solutions to be changed in <10 s without altering tubule pressure or flow. The other half of the theta-glass pipette,

which was fitted with an Ag/AgCl wire and filled with 0.9% NaCl, formed the current-passing limb.

Electrical connections were made to the outflow ends of the perfusate and bathing solutions using free-flowing KCl-Ag/AgCl bridges filled with 3 M KCl. No liquid junction corrections were necessary with this system (Hebert et al., 1984). The transepithelial voltage was measured between the perfusion half of the perfusion pipette and the bath. Voltage at the collecting end was measured with an Ag/AgCl wire connected to a high-impedance electrometer. Voltage deflections in response to biphasic square-wave current pulses of 800 ms duration were read from a strip-chart recorder (Gould 2200S Recorder, Gould, Inc., Cleveland, OH) 100–150 ms after the onset of a current pulse, at which time all pipette capacitance changes were complete. The details of this methodology for the mouse mTALH have been presented previously (Hebert et al., 1984a).

Transepithelial electrical conductances were calculated using modifications of terminated cable equations (Burg et al., 1968; Helman et al., 1971; Helman, 1972) described previously for this laboratory (Hebert et al., 1981a, 1984). The conductances reported

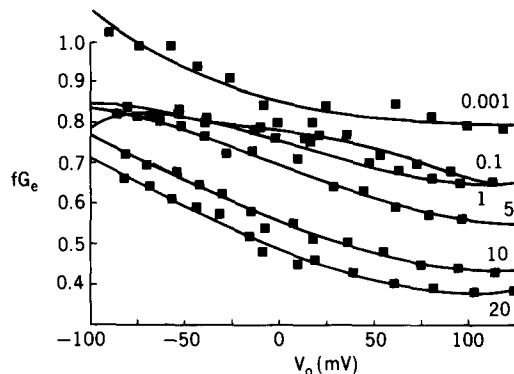


FIGURE 1. Representative experiment illustrating the voltage dependence of the fractional transepithelial conductance, fG_e , for luminal Ba^{2+} concentrations between 0.001 and 20 mM. The transepithelial voltage, V_o , shown on the abscissa, is the input voltage measured during current injection. Each solid line connects fG_e values obtained at the Ba^{2+} concentration (in millimolar) indicated at the right-hand position of the curve. ADH, 10 μ U/ml, was present throughout the experiment; luminal K^+ was omitted during Ba^{2+} additions.

for control conditions in the present studies were the mean conductance values calculated over the range 0–600 nA, since current-voltage relations are linear for this positive current range (Hebert et al., 1984). Na^+ -to- Cl^- permselectivity ratios were determined as described previously (Hebert et al., 1984) from the measurement of zero-current bath-to-lumen dilution voltages according to the Goldman equation.

The Ba^{2+} -mediated blockade of apical membrane K^+ channels in the mouse mTALH is dependent both on the luminal Ba^{2+} concentration and on the magnitude and orientation of the transepithelial voltage during current pulses (Hebert et al., 1984). In the experiments reported in this paper, we wished to assess the concentration dependence of the Ba^{2+} -mediated blockade of the transcellular conductance. Thus, in order to avoid any effects of the voltage imposed across the tubule epithelium during current pulses on the Ba^{2+} blockade, conductances reported in the presence of luminal Ba^{2+} were obtained from stable, minimal conductance values at large, positive current pulses.

The rationale for this procedure is illustrated in Fig. 1 for luminal Ba^{2+} blockade in a single mTALH tubule segment. The Ba^{2+} -inhibited transepithelial conductance, G_e^i , was

calculated at each current pulse, I_o , over the range -600 to $+600$ nA and expressed as the fraction of the control conductance, G_e , obtained at the same current:

$$fG_e = G_e^i/G_e, \quad (1)$$

where fG_e is the conductance ratio at the current I_o .

A plot of fG_e vs. the imposed transepithelial voltage, V_o , at which the experimental conductance was calculated, is shown in Fig. 1. Each curve, drawn by eye, connects fG_e values at the indicated luminal Ba^{++} concentration, expressed in millimoles per liter. It is readily apparent that the curves in Fig. 1 are nonlinear. However, for each luminal Ba^{++} concentration, fG_e reached a stable nadir at lumen-positive voltages of >75 mV. In other words, for imposed lumen-positive voltages of >75 mV, G_e^i and G_e were voltage independent. Thus, conductances reported in the presence or absence of luminal Ba^{++} were obtained from mean conductance values obtained at imposed lumen-positive transepithelial voltages of >75 mV, that is, when the reduction in G_e was maximal for that Ba^{++}

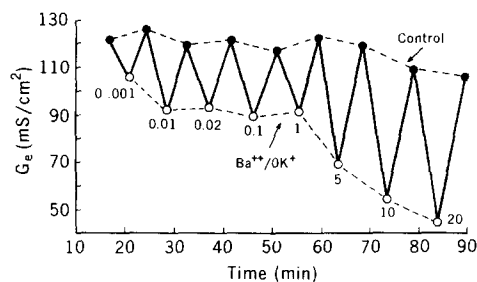


FIGURE 2. Representative experiment showing the protocol for assessing the concentration dependence of luminal Ba^{++} , $0 K^+$ on the transepithelial conductance, G_e . The solid line connects sequential transepithelial conductance values measured in the same tubule: the control G_e values, with luminal $5 mM K^+$, $0 Ba^{++}$, are connected by the upper dotted line; the G_e values obtained in the presence of various concentrations of luminal Ba^{++} with $0 K^+$ are connected by the lower dotted line. Luminal Ba^{++} concentrations (in millimolar) are indicated below the lower circles. Note that each addition of luminal Ba^{++} was followed by a return to the control perfusate ($0 Ba^{++}/5 mM K^+$) and that the control conductances varied by $<10\%$ throughout the experiment. $10 \mu U/ml$ ADH was uniformly present in the bath.

concentration. It should be noted, however, that the present experiments do not provide information about the mechanisms responsible for the voltage dependence of Ba^{++} blockade of transcellular conductance.

Fig. 2 shows the results of a typical experiment illustrating the protocol for assessing the change in G_e upon adding various concentrations of Ba^{++} , and deleting K^+ , in luminal fluids. The experimental sequence depicted by the solid line in Fig. 2 was begun when V_e and G_e had reached their ADH-dependent, steady state maximal values (Hebert et al., 1981a, 1984). The addition of luminal Ba^{++} , over the range 0.001 – 20.0 mM, resulted in rapid reductions in G_e to stable minimal values at each Ba^{++} concentration. A subsequent return to the control perfusate, containing $0 Ba^{++}$, $5 mM K^+$, was followed by rises in G_e (solid squares) to values that varied by $<5\%$ from the pre-barium conductances. Thus, the reductions in G_e , with all concentrations of Ba^{++} tested, were completely reversible, and there was no detectable temporal decline in the control conductance (upper dotted

line in Fig. 2). It is also relevant to note that, in most experiments, the perfusate Ba⁺⁺ concentrations were varied at random, rather than in the stepwise fashion shown in Fig. 2. In other words, the reductions in G_e observed with luminal 0 K⁺ and Ba⁺⁺ addition were time invariant.

The results in Fig. 2 confirm our earlier observations on the magnitude of the reductions in G_e with luminal 0.1 and 5.0 mM Ba⁺⁺ and 0 K⁺ (Hebert et al., 1984; Hebert and Andreoli, 1984c). In addition, the data indicate that luminal Ba⁺⁺ concentrations of >5 mM produced progressively larger reductions in G_e than those observed at lower Ba⁺⁺ concentrations.

The total transepithelial conductance, G_e , is the sum of the shunt conductance, G_s , and the transcellular conductance, G_c ; the K⁺ transference number for apical membranes is, as indicated above, virtually unity (Hebert and Andreoli, 1984c); and luminal Ba⁺⁺, 0 K⁺ affects only the transcellular conductance pathway (Hebert et al., 1984). Thus, in accord with earlier arguments (Hebert and Andreoli, 1984c), the progressive increase in the magnitudes of the differences between the control conductances and those in the presence of increasing concentrations of luminal Ba⁺⁺, at 0 K⁺, represent a progressive decrement in the transcellular conductance, G_c , referable to an increase in the fraction of apical K⁺ channels blocked by Ba⁺⁺.

Morphology

Photographs of the perfused tubules were obtained for the various conditions of perfusate and bath osmolality using a Zeiss IM 45 microscope equipped for differential interference contrast. The general setup was similar to that described previously by Horster and Gundlach (1979); the primary optical elements consisted of a 100× oil objective (1.25 numerical aperture [NA]) and a condenser made from a 40× water immersion lens (0.75 NA), both of which had Wolleston prisms.

Statistical Analyses

Average values from a number of tubules were used to compute a mean ± standard error of the mean (SEM) on the indicated number of tubules (n). The statistical significance for mean paired differences was computed from the distribution.

RESULTS

Concentration Dependence of Luminal Ba⁺⁺ Blockade of the Transepithelial Conductance

Fig. 3 presents the results of experiments with a series of individual tubules in which we assessed the concentration dependence of the luminal Ba⁺⁺, 0 K⁺-mediated blockade of transcellular conductance; the experiments were carried out using the format shown in Fig. 2. The data presented in Fig. 3 demonstrate that the control conductances without luminal Ba⁺⁺, shown by the points on the ordinate, varied between 90 and 120 mS/cm². This degree of variability for control conductances is consistent with earlier results (Hebert and Andreoli, 1984c). Indeed, because of this variability among tubules, paired observations on G_e were made in each tubule. That is, by following the protocol illustrated in Fig. 2, each tubule provided its own internal control.

The data shown in Fig. 3 indicate that 0.001 mM luminal Ba⁺⁺ produced a discernible reduction in G_e , that G_e remained relatively constant in the range 0.001–1.0 mM Ba⁺⁺, and that at luminal Ba⁺⁺ concentrations of >1.0 mM, G_e

fell progressively. The control transepithelial conductance, 110.9 ± 4.4 mS/cm², was virtually identical to that observed previously in the presence of ADH (Hebert et al., 1984). In the presence of luminal 20 mM Ba⁺⁺, 0 K⁺, G_e had a value of 40.4 ± 1.2 mS/cm² ($\Delta G_e = 69.6 \pm 4.3$; $P < 0.001$).

Thus, when taken together, the results in Figs. 2 and 3 indicate, in accord with earlier observations (Hebert et al., 1984), that the fraction of transcellular conductance blocked by the combination of luminal Ba⁺⁺, 0 K⁺ varied with the luminal Ba⁺⁺ concentration. At 20 mM luminal Ba⁺⁺, the residual conductance accounted for only 35% of the total transepithelial conductance, G_e .

The kinetic characteristics of the blockade of G_e by 0 luminal K⁺ with various luminal Ba⁺⁺ concentrations were assessed by plotting the double-reciprocal relation between the fall in transepithelial conductance and various luminal concentrations of Ba⁺⁺ with 0 K⁺. These relations are shown in Fig. 4, using all the experimental data from Fig. 3. The ordinate in Fig. 4 is $1/\Delta G_e^{Ba}$, that is, the reciprocal of the component of transcellular conductance blocked, in a given

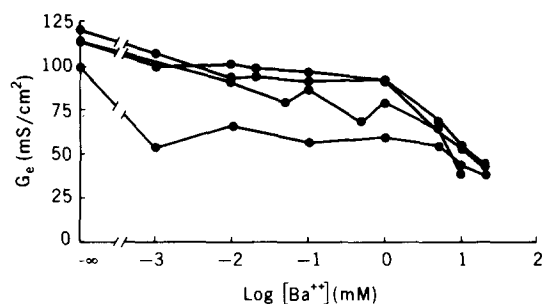


FIGURE 3. Concentration dependence of the transepithelial conductance, G_e , with luminal Ba⁺⁺, 0 K⁺. The lines connect conductance values from individual tubules. The points on the ordinate indicate the control conductance value for each tubule obtained with luminal 0 Ba⁺⁺, 5 mM K⁺. All experiments were conducted in the presence of peritubular ADH at a concentration of 10 μ U/ml.

tubule, at a given concentration of luminal Ba⁺⁺ with 0 K⁺. The abscissa is $1/[Ba^{++}]$. Accordingly, the reciprocal of the zero intercept of these relations provides an estimate of the transcellular conductance at an infinite concentration of luminal Ba⁺⁺ and 0 K⁺.

The results in Fig. 4 show clearly that the relation between $1/\Delta G_e^{Ba}$ and $1/Ba^{++}$ was nonlinear. However, this nonlinear relation could be separated into two linear regions: one for Ba⁺⁺ concentrations between 1 and 20 mM, and another for Ba⁺⁺ concentrations between 0.001 and 1 mM. These results are presented in Fig. 5.

The upper panel of Fig. 5 shows the linear relation between $1/\Delta G_e^{Ba}$ and $1/Ba^{++}$ for the concentration range 0.001–1.0 mM Ba⁺⁺, using the same abscissa as in Fig. 4. The linear relation had a $1/y$ -intercept value of 31.8 ± 1.7 mS/cm². In the lower panel of Fig. 5, we used an expanded abscissa to present the relation between $1/\Delta G_e^{Ba}$ and $1/Ba^{++}$ for the concentration range 1–20 mM Ba⁺⁺. The magnitude of the transcellular conductance calculated from the $1/y$ -intercept

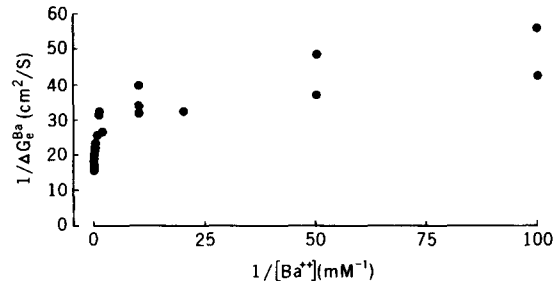


FIGURE 4. A reciprocal plot of the experimental data from Fig. 3.

was 61.8 ± 1.7 mS/cm² (Fig. 5, bottom). The latter value is clearly in close agreement with 69.6 ± 4.3 mS/cm², the transcellular conductance actually estimated from the 20 mM luminal Ba⁺⁺ experiments. Accordingly, it is reasonable to conclude that the combination of luminal 20 mM Ba⁺⁺, 0 K⁺ produced a near-maximal reduction in the transepithelial conductance.

The inhibitory constants (K_i) calculated from the reciprocal relations in Fig. 5 for the two linear regions, 0.001–1.0 and 1–20 mM Ba⁺⁺, were 5.6 ± 1.9 and 900 ± 110 μM, respectively. These results indicate that the K_i for the Ba⁺⁺-mediated blockade of transcellular conductance was >10²-fold greater with 1–20 mM luminal Ba⁺⁺ than with 0.001–1.0 mM Ba⁺⁺.

When taken together, the results in Figs. 3–5 indicate that the blockade of apical membrane K⁺ channels by the combination of luminal Ba⁺⁺ and 0 K⁺ was kinetically complex. The concentration dependence of G_e on luminal Ba⁺⁺ was not monotonic; rather, in the concentration range 0.001–1.0 mM luminal Ba⁺⁺,

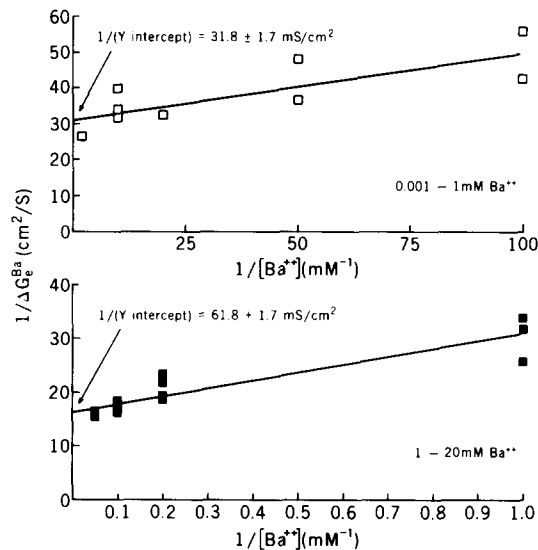


FIGURE 5. (Top) Least-squares linear regression fits for 0.001–1.0 mM Ba⁺⁺ ($r = 0.94$) using the same abscissa as in Fig. 4. (Bottom) Least-squares regression for the 1–20 mM Ba⁺⁺ data in Fig. 4 ($r = 0.94$), using an expanded abscissa.

G_e remained relatively constant, but declined sharply in the concentration range 1–20 mM luminal Ba^{++} (Fig. 3). Similarly, reciprocal plots of the experimental data presented in Fig. 3 yielded two distinct linear regions, one for the 0.001–1.0 mM Ba^{++} concentration range and another for the 1–20 mM Ba^{++} concentration range (Fig. 5). These two linear regions had different y -intercepts (Fig. 5) and yielded K_i values that differed by $>10^2$ -fold. Clearly, these results would obtain if the interactions between luminal Ba^{++} and apical membrane K^+ conductance, in the absence of luminal K^+ , were negatively cooperative.

Completeness of G_e Blockade with Luminal 20 mM Ba^{++} , 0 K^+

The results in Figs. 2 and 3 indicate clearly that increasing concentrations of luminal Ba^{++} , with 0 luminal K^+ , produced a progressively greater reduction in the transepithelial conductance. Several lines of evidence argue that the residual transepithelial conductance in the presence of luminal 20 mM Ba^{++} , 0 K^+ provides a reasonable estimate of the shunt or paracellular conductance. First, at 20 mM Ba^{++} , 0 K^+ , the observed magnitude of the Ba^{++} -sensitive conductance was virtually indistinguishable from that calculated using a double-reciprocal plot of the 1–20 mM luminal Ba^{++} data, at an infinite concentration of luminal Ba^{++} (Fig. 4).

Second, luminal 5 mM Ba^{++} , 0 K^+ does not affect either the electrical permeability ratio (P_{Na}/P_{Cl}) or the passive bath-to-lumen ^{22}Na permeability in the mouse mTALH (Hebert et al., 1984). The reduction in G_e produced by luminal 5 mM Ba^{++} , 0 K^+ was 85–95% of that for 20 mM Ba^{++} , 0 K^+ (Fig. 3). Moreover, the results presented in Fig. 7 (see below) show clearly that, with 20 mM luminal Ba^{++} , 0 K^+ , the P_{Na}/P_{Cl} permselectivity ratio of the shunt pathway was indistinguishable from that found for these tubules without Ba^{++} (Hebert et al., 1984). Thus, we argue that luminal 20 mM Ba^{++} , 0 K^+ affected primarily, if not exclusively, the transcellular conductance pathway.

We should also note in this connection that Halm et al. (1985) have recently found that, in flounder intestinal mucosa, 2 mM luminal Ba^{++} reduced the paracellular conductance by ~3%; these workers also noted that ~96% of the total transepithelial conductance of the flounder intestinal mucosa was paracellular. Obviously, for such a circumstance, the use of luminal Ba^{++} might lead to an erroneous estimate of G_e , as noted by Halm et al. (1985). However, in the mTALH, the transcellular conductance makes up at least 50% of the total electrical conductance (Hebert et al., 1984; Hebert and Andreoli, 1984c; Fig. 3). 5 mM luminal Ba^{++} does not affect, as noted above, either the absolute dissipative permeation rate for $^{22}Na^+$ or the electrical P_{Na}/P_{Cl} ratio (Hebert et al., 1984), but it raises the apical-to-basolateral membrane resistance ratio ~10-fold (Hebert and Andreoli, 1984c). With 20 mM luminal Ba^{++} , the P_{Na}/P_{Cl} selectivity ratio of the paracellular pathway was unaffected (Fig. 7), whereas, as indicated below, the conductance unaffected by 20 mM Ba^{++} was greater than the conductance calculated from dissipative $^{22}Na^+$ and $^{36}Cl^-$ fluxes (Table I). Thus, we conclude that, in the mTALH, any effects of Ba^{++} on the paracellular pathway were trivial with respect to the Ba^{++} effect on transcellular conductance (Fig. 3).

Finally, an argument for the completeness of the blockade of G_c with luminal 20 mM Ba^{++} , 0 K^+ derives from a comparison of the 20 mM Ba^{++} -insensitive G_e with that for the sum of the conductances of ^{22}Na and ^{36}Cl (G_t). These data are shown in Table I. The residual G_e with luminal 20 mM Ba^{++} , 0 K^+ was obtained from 20 mTALH segments (including the 4 from Figs. 3–5) and the value of G_t was computed from the sum of all previously reported measurements of passive bath-to-lumen fluxes of $^{22}Na^+$ and $^{36}Cl^-$. It should be noted in this regard that the comparison of tracer and electrical conductances was deliberately unpaired, since, as noted previously (Hebert et al., 1984), tracer flux and electrical measurements are best carried out with long and short tubule lengths, respectively. The results presented in Table I indicate that the 20 mM Ba^{++} -insensitive G_e was comparable to that for the sum of the conductances for tracer Na^+ and Cl^- , ionic species that constitute >95% of the total shunt conductance (Hebert et al., 1981a).

TABLE I
A Comparison of the 20 mM Ba⁺⁺-insensitive G_e with G_t

G_e (20 mM Ba^{++} , 0 K^+)	G_t (from $^{22}Na^+$ and $^{36}Cl^-$ fluxes)
<i>mS/cm²</i>	<i>mS/cm²</i>
53.8±4.3	32.0±1.5
(n = 20)	(n = 15)

The value of G_t was computed, as described previously (Hebert et al., 1981a), from the sum of all previously reported measurements of passive bath-to-lumen fluxes of $^{22}Na^+$ or $^{36}Cl^-$ in the presence of peritubular ADH (Hebert et al., 1981a, 1984). The G_e values are all the conductances insensitive to luminal 20 mM Ba^{++} , 0 K^+ in the present paper.

Effect of Luminal Hypertonicity on the Electrical Properties of the Shunt Pathway

Fig. 6 presents the results of a series of experiments designed to evaluate the effects of luminal hypertonicity on the electrical shunt conductance. The mTALH tubule segments were perfused and bathed with control isotonic solutions until the ADH-dependent values of G_e and V_e reached steady state values (Hebert et al., 1981a). The perfusate was then changed to one containing 20 mM Ba^{++} , 0 K^+ , a combination that, as noted above, provides an estimate of G_s , the shunt conductance (ordinate in Fig. 6).

The results presented in Fig. 6 show clearly that, in paired observations on individual tubules, increases in the perfusate osmolality produced with urea had a relatively small effect on G_s when the luminal urea concentration was <400 mM. However, at luminal urea concentrations of >400 mM, G_s rose with increasing luminal hypertonicity and was increased dramatically when the perfusate contained 800 mM urea.

Fig. 7 shows the effects of luminal urea on the P_{Na}/P_{Cl} permselectivity ratio of the paracellular pathway; the data are from zero-current salt dilution voltages on the same eight tubules reported in Fig. 6. With luminal 20 mM Ba^{++} , 0 K^+ , and no luminal urea, the P_{Na}/P_{Cl} ratio ranged from 2 to 5, in accord with our

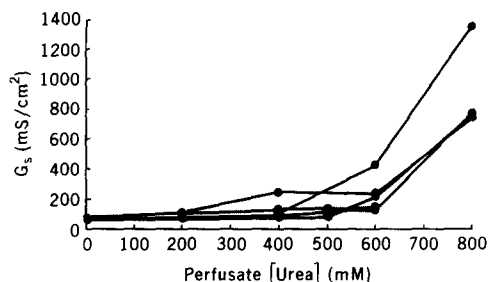


FIGURE 6. The effect of hypertonic perfusate urea on the shunt conductance. G_s values were determined using a perfusate containing 20 mM Ba^{++} , 0 K^+ (Fig. 3) in the presence of bath ADH (solid circles on the ordinate). Urea was added to the perfusate in increments of 200 mM up to a concentration of 800 mM, and the transepithelial conductance was determined at each urea concentration in each tubule (solid circles connected by solid lines).

earlier estimates for the range of electrical P_{Na}/P_{Cl} ratios in these tubules, either with or without luminal Ba^{++} , 0 K^+ (Hebert et al., 1984), or with or without ADH (Hebert et al., 1981a, c). At luminal urea concentrations of <400 mM, the shunt P_{Na}/P_{Cl} ratios varied only slightly from control values; however, with luminal urea concentrations in excess of 400 mM, the shunt P_{Na}/P_{Cl} ratio fell in each of the tubules studied, and converged on a P_{Na}/P_{Cl} ratio in the range of ~ 0.6 at a luminal urea concentration of 800 mM.

The results with either 0 or 800 mM urea are summarized in Table II. With luminal 20 mM Ba^{++} , 0 K^+ , and no luminal urea, G_s and the shunt P_{Na}/P_{Cl} ratio were 70.0 ± 3.3 mS/cm² and 3.14 ± 0.33 , respectively. Both sets of values are in close accord with the values reported previously for G_s (Table I) and the shunt P_{Na}/P_{Cl} ratio (Hebert et al., 1981a, 1984). The addition of 800 mM urea to luminal fluids resulted in a dramatic increase in G_s to 905 ± 150 mS/cm², and in a fall in the P_{Na}/P_{Cl} ratio to 0.62 ± 0.04 . The latter value is indistinguishable from the Na^+/Cl^- mobility ratio in free solution.

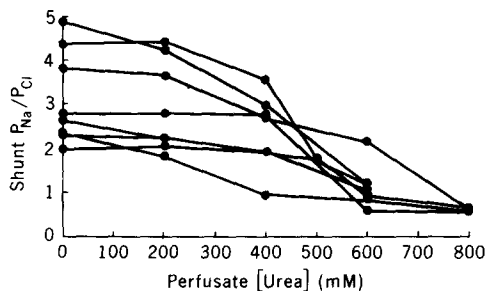


FIGURE 7. The effect of hypertonic perfusate urea on the Na^+/Cl^- permselectivity ratio determined from bath NaCl dilution voltages. The perfusate contained 20 mM Ba^{++} , 0 K^+ throughout, and the perfusate urea concentration was increased in 200-mM increments. P_{Na}/P_{Cl} values for each tubule are connected by solid lines. These data are for the same eight tubules depicted in Fig. 6. Bath ADH at 10 $\mu U/ml$ was present throughout the experiment.

Thus, it is evident that, together with the rise in G_s produced by 800 mM luminal urea, the latter also abolished the characteristics of the junctional complexes responsible for the Na^+/Cl^- permselectivity ratio of ~ 3 seen with isotonic external solutions. Accordingly, it is probable that the rise in G_s produced by luminal hypertonicity in these tubules was due primarily to a rise in electrical conductance through junctional complexes. This conclusion is in accord with the earlier observations of other workers on the effects of luminal hypertonicity on the ionic or nonelectrolyte (Frömter and Diamond, 1972; Lindley et al., 1964; Ussing and Windhager, 1964; Ussing, 1966; DiBona and Civan, 1973; Schafer et al., 1974; de Bermudez and Windhager, 1975) permeability characteristics of other water-impermeant epithelia.

The effects of luminal hypertonicity on the morphology of these tubules are illustrated in Fig. 8. These photographs are from a single in vitro perfused mTALH segment (one of the same tubule segments from which the data in Figs. 6 and 7 and Table II were derived), in which the perfusate urea concentration was sequentially increased from 0 to 800 mM in increments of 200 mM luminal urea. At 200 mM luminal urea, the tubule morphology was indistinguishable

TABLE II
Effects of 800 mM Luminal Urea on G_s and $P_{\text{Na}}/P_{\text{Cl}}$

Luminal urea	G_s	$P_{\text{Na}}/P_{\text{Cl}}$
<i>M</i>	<i>mS/cm²</i>	
0	70.0±3.3	3.14±0.33
800	905±150	0.62±0.04
Δ	835±152 ($P < 0.01$)	2.52±0.41 ($P < 0.01$)

[$n = 8$]

The data are from Figs. 6 and 7. The results are expressed as mean values \pm SEM.

from the control condition. Slight irregularities were observed in the luminal border at 400 mM luminal urea, and these irregularities were clearly distinguishable as blebs and vacuoles at 600 and 800 mM luminal urea (bottom two photographs in Fig. 8). The blebs could not be localized to junctional complexes, because the small cell thickness and narrow interspace width made the cell borders difficult to visualize, even with differential interference contrast viewing. However, the results presented in Fig. 8 are consistent with descriptions of apical vacuoles seen in the toad urinary bladder with mucosal hypertonicity (DiBona, 1978); these vacuoles have been localized to junctional complexes (DiBona, 1978).

One other observation is consistent with an effect of hypertonic perfusate urea on the shunt pathway rather than the transcellular pathway. Specifically, an obvious effect of the addition of Ba^{++} to luminal solutions in these mTALH segments is the "squaring off" of the voltage response at the perfusion pipette to current injection (Hebert et al., 1984). This Ba^{++} -dependent loss of the "long time constant" effect, first noted in gastric mucosa by Kidder and Rehm (1970), is also typical of Ba^{++} -mediated blockade of K^+ channels both in the mouse

mTALH (Hebert et al., 1984a) and in the rabbit cortical collecting duct (Koepen et al., 1983; O'Neil, 1983). In the present studies, we found that 800 mM luminal urea did not alter the squared-off appearance of the input voltage response obtained with luminal 20 mM Ba^{++} , 0 K^+ .

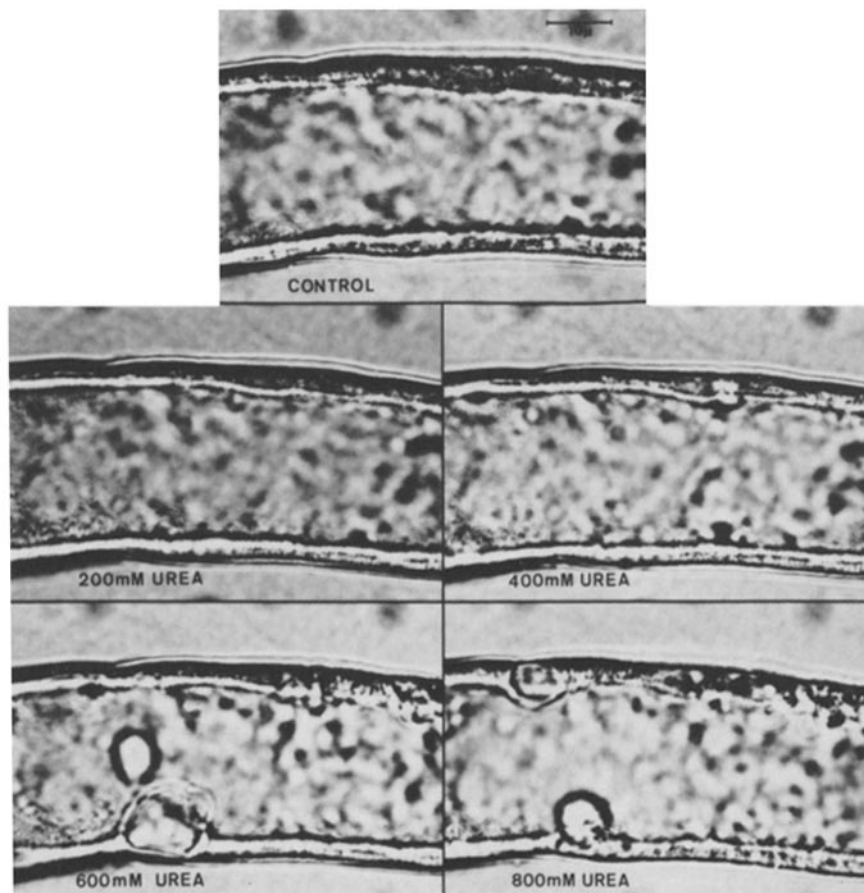


FIGURE 8. The effect of perfusate hypertonicity on mTALH morphology. These photographs of one of the tubules depicted in Figs. 6 and 7 were taken with a 100 \times objective using the differential interference contrast system described in the Materials and Methods. The control perfusate and all subsequent perfusates contained 20 mM Ba^{++} , 0 K^+ . Perfusate urea concentrations are indicated at the bottom of each photograph. Note the irregular luminal border at 400 mM urea and the marked luminal blebs at 600 and 800 mM urea.

Asymmetrical Nature of the Hypertonic Urea Effect on the Shunt Pathway

In earlier studies, we found (Hebert et al., 1981c) that increases in peritubular osmolality alone, or increases in both luminal plus peritubular osmolality, dramatically reduced the rate of net NaCl absorption but had no effect either on the passive permeability coefficient for $^{22}Na^+$ or on the electrical P_{Na}/P_{Cl} ratio.

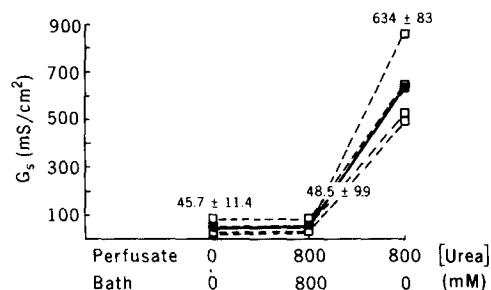


FIGURE 9. The effect of symmetrical vs. asymmetrical bulk solution urea hypertonicity on G_s . All perfusing solutions contained 20 mM Ba⁺⁺, 0 K⁺ and all baths contained a maximal stimulating concentration of ADH (10 μ U/ml). G_s values were obtained with 0 urea, with symmetrical perfusate and bath 800 mM urea (solid squares), and with perfusate 800 mM urea alone (open squares). Conductance values for each tubule ($n = 5$) are connected by dotted lines; the mean values \pm SEM are shown on the figure and are represented by solid lines and solid squares.

However, the results presented in Figs. 6–8 and in Table II indicate that luminal hypertonicity alone increased G_s dramatically and reduced the Na⁺/Cl⁻ permselectivity ratio of the shunt pathway to a value indistinguishable from the Na⁺/Cl⁻ mobility ratio in free solution. It was therefore relevant to inquire whether the latter effects of luminal hypertonicity depended on a transepithelial osmotic gradient from bath to lumen. To test this possibility, we compared the effects of 800 mM urea addition either to the perfusate or to the perfusate plus bath on the shunt conductance, G_s , the electrical P_{Na}/P_{Cl} ratio, and on tubule morphology.

The results of these experiments are presented in Figs. 9–11. As in the case of the data presented in Figs. 6–8, the tubules were mounted in the presence of bath ADH (10 μ U/ml) and the transepithelial conductance was monitored until G_e had attained an ADH-dependent maximal value. Subsequently, the perfusate was switched to luminal 20 mM Ba⁺⁺, 0 K⁺, and the residual conductance was taken to be the shunt conductance, G_s . Paired measurements of G_s and the shunt P_{Na}/P_{Cl} permselectivity ratio were then made in individual tubules in each of three circumstances: (a) without luminal or peritubular urea addition; (b) with

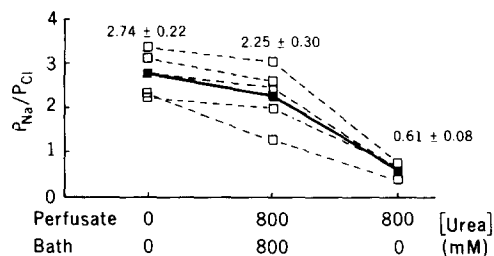


FIGURE 10. Symmetrical vs. asymmetrical bulk solution urea hypertonicity on P_{Na}/P_{Cl} . These data are for the same five tubules depicted in Fig. 9. P_{Na}/P_{Cl} values for each tubule are connected by dotted lines and the mean values \pm SEM, shown on the figure, are depicted by the solid squares connected by a solid line.

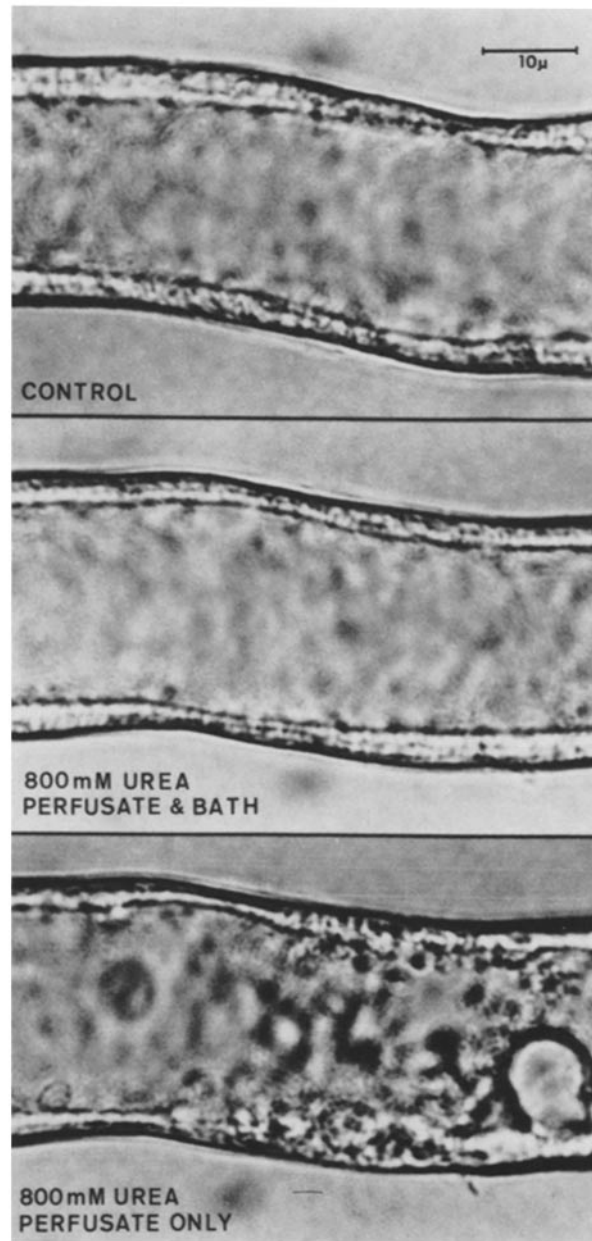


FIGURE 11. Tubule morphology seen under symmetrical (perfusate plus bath) and asymmetrical (perfusate alone) urea hypertonic conditions. The upper photograph shows tubule morphology for control conditions with perfusate 20 mM Ba^{++} , 0 K^+ , 0 urea. Note the smooth luminal border and absence of blebbing in the control condition and with symmetrical 800 mM urea (middle photograph). In contrast, with 800 mM urea only in the perfusate, there is a marked irregularity to the luminal border and large blebs can be seen (lower photograph).

800 mM urea in both luminal and peritubular fluids; and (c) with 800 mM only in luminal solutions.

The data presented in Figs. 9 and 10 show clearly that the symmetrical addition of 800 mM urea to bulk solutions had no significant effect either on G_s (Fig. 9) or on the P_{Na}/P_{Cl} ratio (Fig. 10). These findings are consistent with our previous observations of the effects of combined luminal and peritubular hypertonicity on the passive permeability characteristics of the mouse mTALH (Hebert et al., 1981a). However, in close accord with the results in Figs. 6 and 7, the addition of 800 mM urea only to the perfusate resulted in a large increase in G_s , to 634 ± 83 mS/cm² (Fig. 9), and in a decrease in the P_{Na}/P_{Cl} ratio to 0.61 ± 0.08 (Fig. 10). Moreover, the morphologic observations presented in Fig. 11 indicate that the apical surface bleb formation described in Fig. 8 occurred with luminal urea hypertonicity alone, but not when 800 mM urea was present in both the luminal and peritubular solutions, that is, when the transepithelial osmotic gradient referable to urea was abolished. Thus, when taken together, the results presented in Figs. 6–11 and Table II are consistent with the view that the blebs in apical surfaces, increases in shunt conductance, and decrements in the P_{Na}/P_{Cl} ratio that accompanied luminal hypertonicity were dependent on the simultaneous presence of a transepithelial osmotic gradient from bath to lumen.

DISCUSSION

As indicated in the Introduction, K⁺ is the predominant, and possibly the exclusive, conductive species traversing apical membranes of mouse mTALH segments (Hebert et al., 1984; Hebert and Andreoli, 1984c), as well as other mammalian (Greger, and Schlatter, 1983a, b) and amphibian diluting segments (Guggino et al., 1982; Oberleithner et al., 1982a, b). Moreover, in the mouse mTALH, the combination of luminal Ba⁺⁺ and 0 K⁺ blocks apical K⁺ channels but not the ionic conductances of Na⁺ and Cl⁻ through the paracellular pathway (Hebert et al., 1984). Thus, the experiments reported in this paper were designed to evaluate some characteristics of the blockade of transcellular conductance in mTALH segments by the combination of luminal Ba⁺⁺ and 0 K, and to assess the effects of luminal hypertonicity, coupled with an attendant transepithelial gradient, on the electrical characteristics of the paracellular pathway. Within the limits of experimental error, the data permit the following general conclusions.

Ba⁺⁺ Blockade of G_c

The data in Figs. 1–5 and Table I are consistent with the possibility that the 20 mM Ba⁺⁺-insensitive G_c provided an estimate of the shunt conductance, G_s . According to this view, in these mTALH segments exposed to ADH, ~64% of the total transepithelial conductance was referable to a transcellular conductance. To our knowledge, the magnitudes of G_c and the fractional contribution of G_c to G_e computed for the mTALH from the present experimental data are among the higher values recorded for such data in electrically leaky epithelia. The precise significance of such a large G_c is, as yet, indeterminate. However, it should be noted that the apical membrane K⁺ conductance provides a way for cell-to-lumen recycling of K⁺, which enters cells through an apical Na⁺:K⁺:2 Cl⁻

symport process, and hence contributes to the maintenance of a lumen-positive voltage (Greger and Schlatter, 1983*a, b*; Hebert and Andreoli, 1984*a, c*). In addition, this transcellular K^+ conductance pathway may contribute to the recycling of K^+ in the renal medulla.

The results in Figs. 2–5 indicate that the reduction in G_c referable to Ba^{++} blockade of apical membrane K^+ channels exhibited certain kinetic characteristics typical of negatively cooperative interactions, namely, a rate of decline in G_c that was much less at low (0.001–1.0 mM) than at high (1–20 mM) luminal Ba^{++} concentrations (Figs. 2 and 3), and a considerably smaller K_i at 0.001–1.0 mM luminal Ba^{++} than at 1–20 mM luminal Ba^{++} . The present results, however, provide no definitive explanations for these seemingly negatively cooperative interactions.

Conductance of Lateral Intercellular Spaces

In general, luminal hypertonicity has been noted to have two different kinds of effects on epithelia. In electrically and hydraulically leaky epithelia, luminal hypertonicity, coupled with a transepithelial osmotic gradient, results in a rise in transepithelial electrical resistance (Smulders et al., 1972; Bindslev et al., 1974; Madara, 1983). The latter increase has been attributed either to a collapse of lateral intercellular spaces (Smulders et al., 1972; Bindslev et al., 1974; de Bermudez and Windhager, 1975) or to a luminal hypertonicity-mediated alteration in the architecture of junctional complexes (Madara, 1983). In epithelia that are both electrically tight and relatively water impermeant, luminal hypertonicity produces marked decreases in transepithelial electrical resistance and large increases in junctional complex permeability to water and hydrophilic solutes (Frömter and Diamond, 1972; Lindley et al., 1964; Ussing and Windhager, 1964; Ussing, 1966; DiBona and Civan, 1973; Schafer et al., 1974; de Bermudez and Windhager, 1975). These changes appear to be due to alterations in the structure of junctional complexes that are thought to represent opening of the latter (Erlj and Martínez-Polomo, 1972; DiBona, 1978).

The mouse mTALH is a hybrid epithelium, being electrically leaky but remarkably impermeant to water (Hebert et al., 1981*a*). The experimental results presented in this paper indicate that luminal hypertonicity, and the attendant bath-to-lumen osmotic gradient, considerably diminished the electrical resistance and ionic discriminatory capacity of junctional complexes. This argument is based on three results obtained in tubules in which the transcellular electrical conductance had been blocked by luminal 20 mM Ba^{++} , 0 K^+ : (*a*) the electrical shunt conductance rose appreciably, with luminal urea concentrations in excess of 400 mM (Fig. 6 and Table II); (*b*) simultaneously, the Na^+/Cl^- permselectivity ratio of the paracellular pathway approached that of free solution (Fig. 7 and Table II); and (*c*) with luminal urea concentrations of >400 mM, the apical surfaces formed blebs (Figs. 8 and 11). Clearly, these three results depended on the presence of a transepithelial osmotic gradient, since the combination of 800 mM urea in both luminal and peritubular fluids did not detectably alter the morphology of luminal surfaces (Fig. 11) and had no significant effect on either

the electrical conductance (Fig. 9) or the Na⁺/Cl⁻ permselectivity (Fig. 10) of the paracellular pathway.

It is therefore reasonable to infer that the effects of luminal urea hypertonicity on electrical conductance (Figs. 6 and 9 and Table II) and on transepithelial Na⁺/Cl⁻ permselectivity (Figs. 7 and 10 and Table II) were referable primarily to a striking increase in the conductance of junctional complexes. Obviously, this conclusion is in keeping with earlier conclusions about the effects of luminal hypertonicity on the ionic and nonelectrolyte (Frömter and Diamond, 1972; Lindley et al., 1964; Ussing and Windhager, 1964; Ussing, 1966; DiBona and Civan, 1973; Schafer et al., 1974; de Bermudez and Windhager, 1975) permeabilities of junctional complexes in hydraulically tight epithelia.

Given these considerations, one can argue that the value of G , with 800 mM luminal urea presented in Table II provides a minimal estimate of the ionic conductance of intercellular spaces, exclusive of junctional complexes, during net salt absorption. This estimate, however, is a minimal one. For example, 800 mM luminal urea might not have entirely eliminated the contribution of junctional complexes to the diffusion resistance of the paracellular pathway; alternatively, it could be argued that luminal hypertonicity and the attendant bath-to-lumen osmotic gradient collapsed intercellular spaces (Smulders et al., 1972; DiBona and Civan, 1973; Bindslev et al., 1974; de Bermudez and Windhager, 1975; Madara, 1983), thus increasing their diffusion resistance.

Is V_e Electrogenic?

The spontaneous V_e accompanying net NaCl absorption is, in principle, the sum of at least two terms: V_{elec} , an electrogenic voltage, and V_{dil} , a zero-current dilution voltage referable to salt accumulation in intracellular spaces during salt absorption (Hebert et al., 1981*b*). The results presented in Figs. 1–6 and Table I can be used to make calculations about the average salt concentration in lateral intercellular spaces during ADH-dependent net NaCl absorption in the mTALH, and hence about the relative contributions of V_{elec} and V_{dil} to observed values of V_e . The approach is as follows.

The net rate of salt absorption (J_{NaCl}^{net} [pM/s·cm⁻²]) in isolated mTALH segments exposed to symmetrical external solutions and perfused at rates sufficiently rapid to preclude significant axial changes in solute concentration, is given by the Nernstian form (Hebert et al., 1981*b*):

$$J_{NaCl}^{net} = \frac{2P_{Na}^s P_{Cl}^s}{P_{Na}^s + P_{Cl}^s} (\bar{C}_{NaCl} - C_{NaCl}^b), \quad (2)$$

where P_{Na}^s and P_{Cl}^s are the individual ionic permeability coefficients (centimeters per second) for intercellular spaces exclusive of junctional complexes; C_{NaCl}^b is the bath concentration of NaCl; and \bar{C}_{NaCl} is the average concentration of NaCl in intercellular spaces during net salt absorption. If the Na⁺/Cl⁻ mobility ratio of intercellular spaces is ~0.66, as in free solutions, we have:

$$P_{Na}^s \cong 0.66 P_{Cl}^s, \quad (2a)$$

and if the values of G_s with 800 mM luminal urea (Table II) provide a minimal estimate of the ionic conductances of paracellular spaces, exclusive of junctional complexes, P_{Cl}^s can be expressed as:

$$P_{Cl}^s = 0.66 G_s^{urea} \left(\frac{RT}{F^2} \right) / C_{NaCl}^b, \quad (3)$$

where G_s^{urea} is the conductance with luminal 800 mM urea, 20 mM Ba^{++} , and 0 K^+ (Table II) and, in all experiments, C_{NaCl}^b equals the bath NaCl concentration (Hebert et al., 1981*b*, 1984).

The ADH-dependent values for J_{NaCl}^{net} in these mTALH segments vary with V_e , but in more than 100 mouse mTALH tubule segments studied in this laboratory to date, the maximal measured value for the ADH-dependent J_{Cl}^{net} was $\sim 10^4$ $peq/s \cdot cm^{-2}$ or a J_{NaCl}^{net} of 10^4 $pmol/s \cdot cm^{-2}$, at a V_e of ~ 10 mV (Hebert et al., 1981*a-c*, 1984). By using a J_{NaCl}^{net} value of 10^4 $pM/s \cdot cm^{-2}$, $C_{NaCl}^b = 145$ mM (see Materials and Methods), and a G_s^{urea} of 905 mS/cm^2 (Table II), Eqs. 2, 2*a*, and 3 yield:

$$\bar{C}_{NaCl} = 150.7 \text{ mM.}$$

Thus, for junctional complexes that, during net NaCl absorption, are approximately three times more permeable to Na^+ than Cl^- (Table II), V_{dil} , calculated as described previously (Hebert et al., 1981*b*), would contribute only ~ 0.7 mV to the observed V_e of 10 mV.

Obviously, the calculations indicated above might have overestimated or underestimated V_{dil} . If, for example, \bar{C}_{NaCl} was less than indicated above, V_{dil} would be < 0.7 mV. We emphasize in this regard that the values of P_{Na}^s and P_{Cl}^s computed from Eqs. 2*a* and 3 provide a minimal estimate of the conductance of intercellular spaces, exclusive of junctional complexes, since, as noted above, at least two factors, singly or in unison, might have resulted in a minimum estimate of G_s^{urea} in Eq. 3, namely, 800 mM luminal urea might not have opened junctional complexes entirely, and/or 800 mM luminal urea might have collapsed partially intercellular spaces.

Alternatively, the results presented in Table I indicate that the G_s insensitive to 20 mM luminal Ba^{++} was ~ 22 mS/cm^2 greater than G_t ; thus, 20 mM luminal Ba^{++} might not have blocked ~ 20 – 25 mS/cm^2 of the transcellular conductance. Consequently, the true value of G_s^{urea} (Eq. 3) may have been 20–25 mS/cm^2 less than the value of 905 mS/cm^2 reported in Table II. Even for such a circumstance, however, V_{dil} calculated as described above would have contributed only 1.1 mV to the observed V_e of 10 mV.

Thus, we argue from these considerations that, in these mTALH segments, V_e is entirely, or almost entirely, transcellular. This conclusion is in keeping with our earlier argument about the electrogenic nature of V_e (Hebert et al., 1984).

Ratio of Net Paracellular Na^+ Flux to Net Cl^- Absorption

It has been proposed that net NaCl absorption in the mouse mTALH (Hebert et al., 1984), as well as in other mammalian TALH segments (Murer and Greger, 1982), involves an electroneutral $Na^+ : K^+ : 2 Cl^-$ apical membrane entry step. We have argued (Hebert et al., 1984) that a significant fraction of net Na^+ absorption

might be driven paracellularly by V_e , if the latter were electrogenic. The results presented in the preceding section, namely, that V_e is electrogenic, provide support for the latter argument. Thus, for a constant stoichiometry of the $\text{Na}^+:\text{K}^+:2\text{Cl}^-$ entry, the ratio of net Cl^- absorption ($J_{\text{Cl}}^{\text{net}}$) to net Na^+ absorption through the paracellular pathway (shunt $J_{\text{Na}}^{\text{net}}$) should have a value of 2.0.

However, the results presented in Figs. 6 and 7, as well as those in earlier studies (Hebert et al., 1981a, 1984; Hebert and Andreoli, 1984b), indicate clearly that there is a considerable degree of variation in the variables G_e , G_s , and $P_{\text{Na}}/P_{\text{Cl}}$ from tubule to tubule. Consequently, we developed an approach in which the ratio of net transcellular Cl^- absorption to net paracellular Na^+ absorption could be expressed in terms of a series of variables that could be estimated in each tubule studied. The major assumptions are as follows.

The major conducting species crossing apical membranes is K^+ (Hebert et al., 1984; Hebert and Andreoli, 1984b). Accordingly, net transcellular K^+ secretion is accompanied by secretory Cl^- flux through the paracellular route ($J_{\text{Cl}}^{\text{shunt}}$). Furthermore, the results presented in the previous section indicate that V_e is electrogenic. In empirical terms, we found previously (Hebert et al., 1984), from direct measurements, that:

$$J_e = J_{\text{Cl}}^{\text{net}} + J_{\text{K}}^{\text{net}}, \quad (4)$$

where $J_{\text{Cl}}^{\text{net}}$ is the measured rate of net Cl^- absorption; $J_{\text{K}}^{\text{net}}$ is the measured rate of net K^+ secretion; and J_e , the equivalent short-circuit current, is:

$$J_e = G_e V_e / F, \quad (4a)$$

where F is the Faraday constant.

Thus, $J_{\text{Cl}}^{\text{shunt}}$ can be expressed as:

$$J_{\text{Cl}}^{\text{shunt}} = \frac{G_s V_e}{F} \left(\frac{P_{\text{Cl}}}{P_{\text{Na}} + P_{\text{Cl}}} \right), \quad (5)$$

where G_s , the shunt conductance, is the component of G_e insensitive to luminal 20 mM Ba^{++} , 0 K^+ (Fig. 1), and V_e is the spontaneous transepithelial voltage during net salt absorption. Similarly, the dissipative net absorptive flux of Na^+ (shunt $J_{\text{Na}}^{\text{net}}$) is:

$$\text{shunt } J_{\text{Na}}^{\text{net}} = \frac{G_s V_e}{F} \left(\frac{P_{\text{Na}}}{P_{\text{Na}} + P_{\text{Cl}}} \right). \quad (6)$$

By combining Eqs. 4–6, we obtain:

$$J_{\text{Cl}}^{\text{net}} / \text{shunt } J_{\text{Na}}^{\text{net}} = \frac{J_e - G_s V_e / F \left(\frac{P_{\text{Cl}}}{P_{\text{Na}} + P_{\text{Cl}}} \right)}{G_s V_e / F \left(\frac{P_{\text{Na}}}{P_{\text{Na}} + P_{\text{Cl}}} \right)}, \quad (7)$$

and by rearranging into a linear form, we obtain:

$$\frac{G_e F (1 + P_{\text{Na}}/P_{\text{Cl}})}{G_s} = \frac{J_{\text{Cl}}^{\text{net}}}{\text{shunt } J_{\text{Na}}^{\text{net}}} (P_{\text{Na}}/P_{\text{Cl}}) + 1. \quad (8)$$

The left-hand term of Eq. 8 contains the electrical variables G_e , G_s , and P_{Na}/P_{Cl} . For a constant stoichiometry of net Cl^- absorption to net shunt Na^+ absorption driven by an electrogenic V_e , there should be a linear relation, with a zero intercept of unity, between the left-hand term of Eq. 8 and the P_{Na}/P_{Cl} ratio. To test this relation, we used the following variables, which were measured in the same tubule presented in Figs. 6–11: G_e , P_{Na}/P_{Cl} , V_e , and J_e , with 20 mM luminal K^+ , 0 Ba^{++} , and 10 $\mu U/ml$ bath ADH, and G_s and P_{Na}/P_{Cl} , with luminal 20 mM Ba^{++} , 0 K^+ , and 10 $\mu U/ml$ bath ADH.

Fig. 12 shows the results in these 13 tubules plotted according to Eq. 8. The abscissa indicates that the P_{Na}/P_{Cl} selectivity ratio varies from 2 to 5, in accord with the degree of variability for this measurement indicated in Fig. 2 and reported previously (Hebert et al., 1981a, 1984). Fig. 7 also shows that, over this range of P_{Na}/P_{Cl} values, the relation was linear ($r = 0.93$), with an intercept of 1.13 ± 0.25 at a P_{Na}/P_{Cl} ratio of 0; this value is obviously in close accord with that predicted for the left-hand term of Eq. 8 at a P_{Na}/P_{Cl} value of 0.

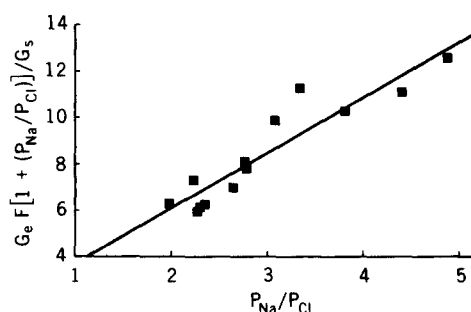


FIGURE 12. Determination of the ratio of net Cl^- absorption (J_{Cl}^{net}) to net Na^+ absorption through the paracellular pathway (shunt J_{Na}^{net}) for all 13 tubules, where V_e , G_e , G_s , and the P_{Na}/P_{Cl} ratio were determined. The $J_{Cl}^{net}/\text{shunt } J_{Na}^{net}$ ratio is represented by the slope of the relation according to Eq. 8. $J_{Cl}^{net}/\text{shunt } J_{Na}^{net} = 2.4 \pm 0.3$; y -intercept = 1.31 ± 0.25 ; $r = 0.93$; $P < 0.0001$; $n = 13$.

For a constant stoichiometry of electroneutral $Na^+ : K^+ : 2 Cl^-$ entry and an electrogenic V_e , there must also be a constant ratio of 2 between J_{Cl}^{net} and the shunt component of net Na^+ absorption. In this regard, the results presented in Fig. 7 indicate that, in a series of 13 tubules where the P_{Na}/P_{Cl} ratio varied considerably from tubule to tubule, the ratio $J_{Cl}^{net}/\text{shunt } J_{Na}^{net}$ was reasonably constant at 2.4 ± 0.3 . Thus, we argue that an apical $Na^+ : K^+ : 2 Cl^-$ stoichiometry may be a constant characteristic of these tubule segments. According to this view, the variables G_e and G_s and the P_{Na}/P_{Cl} ratio may be intrinsically related, in a given tubule, in such a way as to maintain constant both the $Na^+ : K^+ : 2 Cl^-$ stoichiometry of apical salt entry and the $J_{Cl}^{net}/\text{shunt } J_{Na}^{net}$ ratio.

We acknowledge the able technical assistance of Mr. Marvin Chang and the able secretarial assistance of Ms. Dot Cowan and Ms. Clementine Whitman.

The studies reported in this paper were supported by research grants from the National Institutes of Health (5 ROI AM-25540), and by an American Heart Grant-in-Aid (831294). S.C.H. is an Established Investigator of the American Heart Association (83-259).

Original version received 17 January 1985 and accepted version received 23 December 1985.

REFERENCES

- Bindslev, M., J. M. Tormey, and E. M. Wright. 1974. The effects of electrical and osmotic gradients on lateral intercellular spaces and membrane conductance in a low resistance epithelium. *Journal of Membrane Biology*. 19:357-380.
- Burg, M. B. 1982. Thick ascending limb of Henle's loop. *Kidney International*. 22:454-464.
- Burg, M. B., L. Isaacson, J. Grantham, and J. Orloff. 1968. Electrical properties of isolated perfused rabbit renal tubules. *American Journal of Physiology*. 215:788-794.
- de Bermudez, L., and E. E. Windhager. 1975. Osmotically induced changes in electrical resistance of distal tubules of rat kidney. *American Journal of Physiology*. 229:1536-1546.
- DiBona, D. R. 1978. Direct visualization of epithelial morphology in the living amphibian urinary bladder. *Journal of Membrane Biology. Special Issue*. 45-70.
- DiBona, D. R., and M. M. Civan. 1973. Pathways for movement of ions and water across toad urinary bladder. I. Anatomic site of transepithelial shunt pathways. *Journal of Membrane Biology*. 12:101-128.
- Erlj, D., and A. Martinez-Palomo. 1972. Opening of tight junctions in frog skin by hypertonic urea solutions. *Journal of Membrane Biology*. 9:229-240.
- Frömter, E., and J. Diamond. 1972. Route of passive ion permeation in epithelia. *Nature New Biology*. 235:9-13.
- Greger, R. 1981. Coupled transport of Na⁺ and Cl⁻ in the thick ascending limb of Henle's loop of rabbit nephron. *Scandinavian Journal of Audiology*. 14(Suppl.):1-15.
- Greger, R., and E. Schlatter. 1983a. Cellular mechanism of the action of loop diuretics on the thick ascending limb of Henle's loop. *Klinische Wochenschrift*. 61:1019-1027.
- Greger, R., and E. Schlatter. 1983b. Properties of the lumen membrane of the cortical thick ascending limb of Henle's loop of rabbit kidney. *Pflügers Archiv European Journal of Physiology*. 396:315-322.
- Guggino, W. B., B. A. Stanton, and G. Giebisch. 1982. Regulation of apical potassium conductance in the isolated early distal tubule of the *Amphiuma* kidney. *Biophysical Journal*. 37:338a. (Abstr.)
- Halm, D. R., E. J. Krasny, and R. A. Frizzell. 1985. Electrophysiology of flounder intestinal mucosa. I. Conductance properties of cellular and paracellular pathways. *Journal of General Physiology*. 85:843-864.
- Hebert, S. C., and T. E. Andreoli. 1984a. Control of NaCl transport in the thick ascending limb. *American Journal of Physiology*. 246:F745-F756.
- Hebert, S. C., and T. E. Andreoli. 1984b. Kinetic analysis of Ba⁺⁺-blockade of apical membrane K⁺-channels in mouse medullary thick ascending limbs. *Abstracts of the IXth International Congress of Nephrology*. 416A.
- Hebert, S. C., and T. E. Andreoli. 1984c. Effects of antidiuretic hormone on cellular conductance pathways in mouse medullary thick ascending limbs of Henle. II. Determinants of the ADH-mediated increases in transepithelial voltage and in net Cl⁻ absorption. *Journal of Membrane Biology*. 80:221-233.
- Hebert, S. C., R. M. Culpepper, and T. E. Andreoli. 1981a. NaCl transport in mouse medullary thick ascending limbs. I. Functional nephron heterogeneity and ADH-stimulated NaCl cotransport. *American Journal of Physiology*. 241:F412-F431.
- Hebert, S. C., R. M. Culpepper, and T. E. Andreoli. 1981b. NaCl transport in mouse medullary thick ascending limbs. II. ADH enhancement of transcellular NaCl cotransport; origin of transepithelial voltage. *American Journal of Physiology*. 241:F432-F442.

- Hebert, S. C., R. M. Culpepper, and T. E. Andreoli. 1981c. NaCl transport in mouse medullary thick ascending limbs. III. Modulation of the ADH effect by peritubular osmolality. *American Journal of Physiology*. 241:F443–F451.
- Hebert, S. C., P. A. Friedman, and T. E. Andreoli. 1984. The effects of antidiuretic hormone on cellular conductive pathways in mouse medullary thick ascending limbs of Henle. I. ADH increases transcellular conductance pathways. *Journal of Membrane Biology*. 80:201–219.
- Helman, S. I. 1972. Determination of electrical resistance of the isolated cortical collecting tubule and its possible anatomic location. *Yale Journal of Biology and Medicine*. 45:339–345.
- Helman, S. I., J. J. Grantham, and M. B. Burg. 1971. Effect of vasopressin on electrical resistance of renal cortical collecting tubules. *American Journal of Physiology*. 220:1825–1832.
- Horster, M., and H. Gundlach. 1979. Application of differential interference contrast with inverted microscopes to the *in vitro* perfused nephron. *Journal of Microscopy*. 117:375–379.
- Kidder, G. W., III, and W. S. Rehm. 1970. A model for the long time-constant transient voltage response to current in epithelial tissue. *Biophysical Journal*. 10:215–236.
- Koeppen, B. M., B. A. Biagi, and G. H. Giebisch. 1983. Intracellular microelectrode characterization of the rabbit cortical collecting duct. *American Journal of Physiology*. 244:F35–F47.
- Lindley, B. D., T. Hoshiko, and D. E. Leb. 1964. Effects of D₂O osmotic gradients on potential and resistance of the isolated frog skin. *Journal of General Physiology*. 47:773–793.
- Madara, J. L. 1983. Increases in guinea pig small intestinal transepithelial resistance induced by osmotic loads are accompanied by rapid alterations in absorptive-cell tight-junction structure. *Journal of Cell Biology*. 97:125–136.
- Murer, H., and R. Greger. 1982. Membrane transport in the proximal tubule and thick ascending limb of Henle's loop: mechanisms and their alterations. *Klinische Wochenschrift*. 60:1103–1113.
- Oberleithner, H., W. Guggino, and G. Giebisch. 1982a. Mechanism of distal tubular chloride transport in *Amphiuma* kidney. *American Journal of Physiology*. 242:F331–F339.
- Oberleithner, H., W. Guggino, and G. Giebisch. 1982b. The effect of furosemide on luminal sodium, chloride and potassium transport in the early distal tubule of *Amphiuma* kidney. *Pflügers Archiv European Journal of Physiology*. 396:27–33.
- O'Neil, R. G. 1983. Voltage-dependent interactions of barium and cesium with the potassium conductance of the cortical collecting duct apical cell membrane. *Journal of Membrane Biology*. 74:165–173.
- Schafer, J. A., S. L. Troutman, and T. E. Andreoli. 1974. Osmosis in cortical collecting tubules. ADH-independent osmotic flow rectification. *Journal of General Physiology*. 64:228–240.
- Smulders, A. P., J. M. Tormey, and E. M. Wright. 1972. Effect of osmotically induced water flows on the permeability and ultrastructure of the rabbit gallbladder. *Journal of Membrane Biology*. 7:164–197.
- Ussing, H. H. 1966. Anomalous transport of electrolytes and sucrose through the isolated frog skin induced by hypertonicity of the outside bathing solution. *Annals of the New York Academy of Sciences*. 137:543–555.
- Ussing, H. H., and E. E. Windhager. 1964. Nature of shunt path and active sodium transport path through frog skin epithelium. *Acta Physiologica Scandinavica*. 61:484–504.